JOURNAL OF GEOPHYSICAL RESEARCH, VOL. 111, D23S32, doi:10.1029/2006JD007340, 2006

Single-particle mass spectrometry of tropospheric aerosol particles

D. M. Murphy,[1] D. J. Cziczo,[1,2,3] K. D. Froyd,[1,2] P. K. Hudson,[1,2,4] B. M. Matthew,[1,2,5] A. M. Middlebrook,[1] R. E. Peltier,[6] A. Sullivan,[6] D. S. Thomson,[1,2] and R. J. Weber[6]

Received 23 March 2006; revised 30 June 2006; accepted 24 July 2006; published 30 September 2006.

[1] The Particle Analysis by Laser Mass Spectrometry (PALMS) instrument has measured the composition of single particles during a number of airborne and ground-based campaigns. In the regions studied, 30% to over 80% of the aerosol mass in the free troposphere was carbonaceous material. Most of this carbonaceous material was probably organic. Although there were variations in their amounts, over 90% of accumulation mode particles away from local sources were internal mixtures of sulfates and carbonaceous material. Within this internal mixing, there was variation in the pattern of carbonaceous peaks in the spectra, especially in peaks related to organic acids. Particles with a biomass burning signature were a significant fraction of accumulation mode particles even far from fires. The accumulation mode near the ocean surface off the coasts of California and New England had significant numbers of carbonaceous-sulfate particles whereas at Cape Grim, Tasmania, the organic-sulfate particles were apparently all smaller than 160 nm. Three kinds of nitrate were evident: on mineral particles, on carbonaceous-sulfate particles when the sulfate was fully neutralized, and at temperatures below about 198 K. Most mineral particles showed evidence of the uptake of nitrates and chloride. A peak that probably represents protonated pyridine appears in some spectra in the free troposphere.

Citation: Murphy, D. M., D. J. Cziczo, K. D. Froyd, P. K. Hudson, B. M. Matthew, A. M. Middlebrook, R. E. Peltier, A. Sullivan, D. S. Thomson, and R. J. Weber (2006), Single-particle mass spectrometry of tropospheric aerosol particles, *J. Geophys. Res.*, *111*, D23S32, doi:10.1029/2006JD007340.

1. Introduction

[2] The chemical composition of aerosol particles in the atmosphere is important for a number of reasons. Without attempting a complete review, a few of the reasons are: understanding the atmospheric budgets of aerosols and the associated light scattering [e.g., *Hegg et al.*, 1997; *Kinne et al.*, 2005], the impact of chemical composition on the cloud nucleating ability of particles [*McFiggans et al.*, 2005b], and the impact of heterogeneous chemistry on gas phase species [e.g., *Sommariva et al.*, 2004; *Haggerstone et al.*, 2005; *Larmarque et al.*, 2005; *Ravishankara*, 2005].

[3] A variety of methods have been used on aircraft to measure the chemical composition of particles. Filter sampling is among the most accurate techniques for chemical composition. Ion chromatograph measurements of extracts from airborne filter samples have a long history [e.g., *Lazrus and Gandrud*, 1974; *Huebert et al.*, 1998; *Dibb et al.*, 2003]. Organics have been measured using either thermal analysis of carbon released from filter samples [*Novakov et al.*, 1997] or infrared spectroscopy of concentrated impactor samples [*Maria et al.*, 2003]. Electron microscope analysis allows distinguishing the components of individual particles at a very fine level [e.g., *Posfai et al.*, 1999; *Okada et al.*, 2001; *Krejci et al.*, 2004]. The use of mass spectrometers to measure the composition of atmospheric aerosols was recently reviewed by *Sullivan and Prather* [2005], so a comprehensive reference list will not be attempted here.

[4] With filter and impactor samples, the sample times tend to be long enough that the aircraft flies tens to hundreds of km during a single sample. Also, the samples are generally warmed to room or aircraft cabin temperature before analysis. This warming may be over 100 K for samples acquired near the tropopause, possibly disturbing the composition. The Particle Analysis by Laser Mass Spectrometry (PALMS) instrument provides a unique combination of capabilities for the airborne measurement of aerosol chemistry. Prior to 2005, it was the only instrument on board an aircraft that could analyze more than one component of single particles. Particle evaporation is reduced by in situ analysis on the airplane with short residence times above ambient temperature. PALMS measures nearly all components of aerosols from volatiles to refractory elements, including sulfates, nitrates, carbonaceous material, sea salt, and minerals. Single-particle measurements allow examination of how

[1]Earth System Research Laboratory, NOAA, Boulder, Colorado, USA.
[2]Also at Cooperative Institute for Research in the Environmental Sciences, Boulder, Colorado, USA.
[3]Now at Eidgenössische Technische Hochschule, Zurich, Switzerland.
[4]Now at Department of Chemistry, University of Iowa, Iowa City, Iowa, USA.
[5]Now at Hach Company, Loveland, Colorado, USA.
[6]School of Earth and Atmospheric Sciences, Georgia Institute of Technology, Atlanta, Georgia, USA.

0148-0227/06/2006JD007340$09.00

Table 1. Configurations of the PALMS Single-Particle Instrument

Mission	Primary Location	Aircraft	Most Flights During	Usable Mass Spectra	Sample and Vacuum Inlet	Aerodynamic Sizing?	Mission Notes
WAM	Houston, Texas	WB-57F	Apr–May 1998	27967	capillary	no	high-altitude aerosols
ACCENT	Houston, Texas	WB-57F	Sep 1999	23139	capillary	no	includes rocket plume intercept
Supersite	Atlanta	ground	Aug 1999	489470	capillary	no	
ACCENT2000	Houston, Texas	WB-57F	Sep 2000	46268	capillary	no	
ITCT 2k2	Monterey, California	NOAA P3	Apr-May 2002	275782	CVI (no counterflow) and focusing	no	Asian transport; PILS onboard
CRYSTAL-FACE	Key West, Florida	WB-57F	Jul 2002	14425	CVI and focusing	a few	convective outflow emphasis
Pre-AVE	Houston and San Jose, Costa Rica	WB-57F	Jan–Feb 2004	43735	forward probe and focusing	majority	upper tropical troposphere
NEAQS-ICARTT	Portsmouth, New Hampshire	NOAA P3	Jul–Aug 2004	582861	CVI and focusing	majority	N. American transport; AMS, PILS
CR- AVE	San Jose, Costa Rica	WB-57F	Jan–Feb 2006	65887	CVI and focusing	majority	upper tropical troposphere

particles are mixed. Each particle is sampled at a well-defined time, facilitating comparison with fast response gas phase measurements. The primary disadvantage is that the results are not as quantitative as, for example, filter measurements. Recently, a Particle Into Liquid Sampler (PILS) [*Weber et al.*, 2001; *Y. N. Lee et al.*, 2003] and an Aerodyne Aerosol Mass Spectrometer (AMS) [*Jayne et al.*, 2000; *Bahreini et al.*, 2003] have been flown on aircraft, including the NOAA P3 with PALMS. The 2004 study was the first time that an airborne PILS water-soluble organic carbon (WSOC) analyzer was deployed (A. P. Sullivan et al., Airborne measurements of carbonaceous aerosol soluble in water over northeastern U. S. A.: Method development and an investigation into WSOC sources, submitted to *Journal of Geophysical Research*, 2006). Some comparisons between PALMS and these instruments are presented later in this paper.

2. PALMS Instrument Configurations

[5] The PALMS aircraft instrument was described by *Thomson et al.* [2000]. Briefly, air is brought into the aircraft nose or wing pod through a 5 cm duct at approximately aircraft speed (100 to 200 m s^{-1}). The core of this flow is sampled to bring particles to the instrument, where the sample flow enters the vacuum system through a differentially pumped vacuum inlet. Particles that cross a continuous laser beam cause a burst of scattered light that triggers an excimer laser. The excimer laser beam ablates and ionizes some of the particle and the resulting ions are analyzed with a time of flight mass spectrometer. Either positive or negative ions may be analyzed from each particle. We usually express the size of peaks as fractions of the total number of ions for a given particle. This is because for similar particles the relative peak sizes have been found to be more consistent than the absolute number of ions formed from the laser pulse.

[6] The lower size limit for analysis by PALMS is set by the signal-to-noise ratio of the trigger signal. The smallest particles that could be detected even with low efficiency were 120 to 200 nm, depending on the flight, and particles larger than 250 or 300 nm were readily detected. The upper size limit was set largely by inlet transmission efficiency and was usually over 2 μm. Particles large enough to be measured by PALMS include most of the mass of particles in the free troposphere and a significant fraction of the surface area but not most of the number.

[7] A number of minor changes have been made to the instrument between different missions, including different inlets and the addition of a second laser beam for aerodynamic particle sizing. Table 1 summarizes these changes as well as some overall features of the different missions. PALMS has flown in the nose of the NASA WB57F and in a wing pod on the NOAA P3. Some of the properties of the various inlets are as follows: From 1998 to 2001, PALMS used a 30 cm long capillary that went directly from the duct into the vacuum. The residence time in the capillary was about 5 ms, with a complicated temperature profile that starts with heating due to the aircraft velocity and changes to a mixture of adiabatic cooling and heat conduction from the walls further down the capillary. In 2002 and part of 2004 a counterflow virtual impactor (CVI) inlet was used. The flows were switched every few minutes from cloud nucleus (with counterflow at the inlet tip) to interstitial (air drawn in at the inlet tip) modes except during the ITCT mission, when the cloud nucleus mode was not used. In order to evaporate ice, in cloud nucleus mode the residence time was about 400 ms at either about 280 K for the WB-57F or about 10 K above ambient for the P3. In interstitial mode the temperatures were similar but the residence time was reduced to about 100 ms to limit loss of volatiles. There was about 50 ms of additional residence time in tubing to PALMS at the aircraft nose temperature, usually 250 to 285 K. For the 2004 Pre-AVE mission there was a simple forward pointing inlet inside the 5 cm duct with a short conductive coated Teflon tube going to the instrument. The residence time for this inlet was 10 to 50 ms at nose temperature (typically 250 to 275 K). For the CVI and forward probe inlets, a separate aerodynamic focusing inlet was used to bring the particles into the vacuum system. The design, based on *Schreiner et al.* [1999], had a residence time of about 20 ms and a lower cut point below the smallest particles detected by PALMS.

[8] The capillary inlet, with the shortest residence time and least heating, was best at measuring the most volatile species such as nitrate condensed on particles at ambient temperatures below 198 K [*Murphy and Thomson*, 2000]. However, there were not obvious differences in the overall carbon to sulfate ratios between the various inlets, so at least a fair portion of the carbonaceous aerosol species must survive a

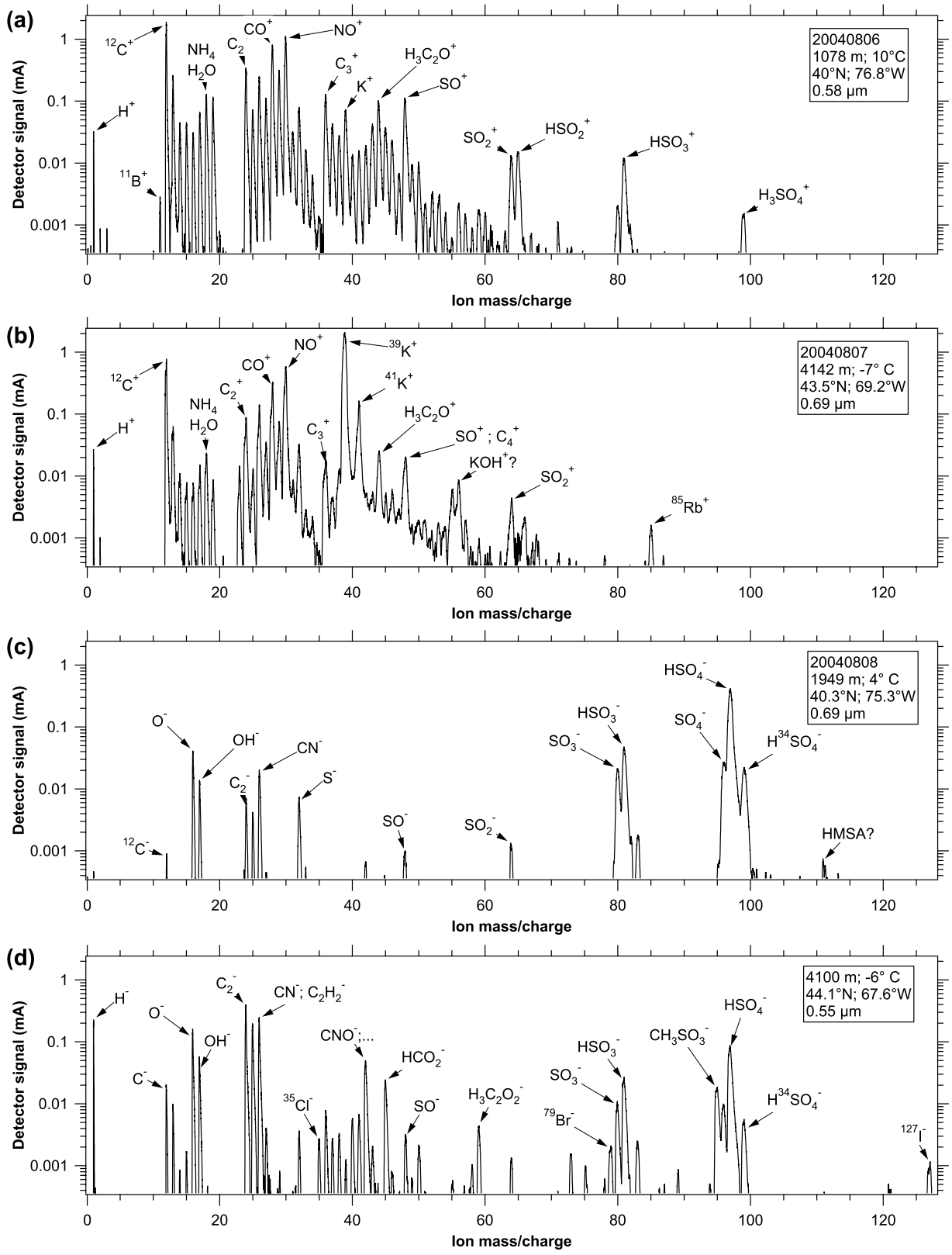

Figure 1. Examples of the most common mass spectra of single particles in (a and b) positive and (c and d) negative ion mode. The two positive ion spectra are distinguished by the large K^+ peak and relatively less sulfate in Figure 1b, indicative of biomass burning particles. These single-particle spectra were chosen to be very close to the average of objectively determined clusters [*Murphy et al.*, 2003].

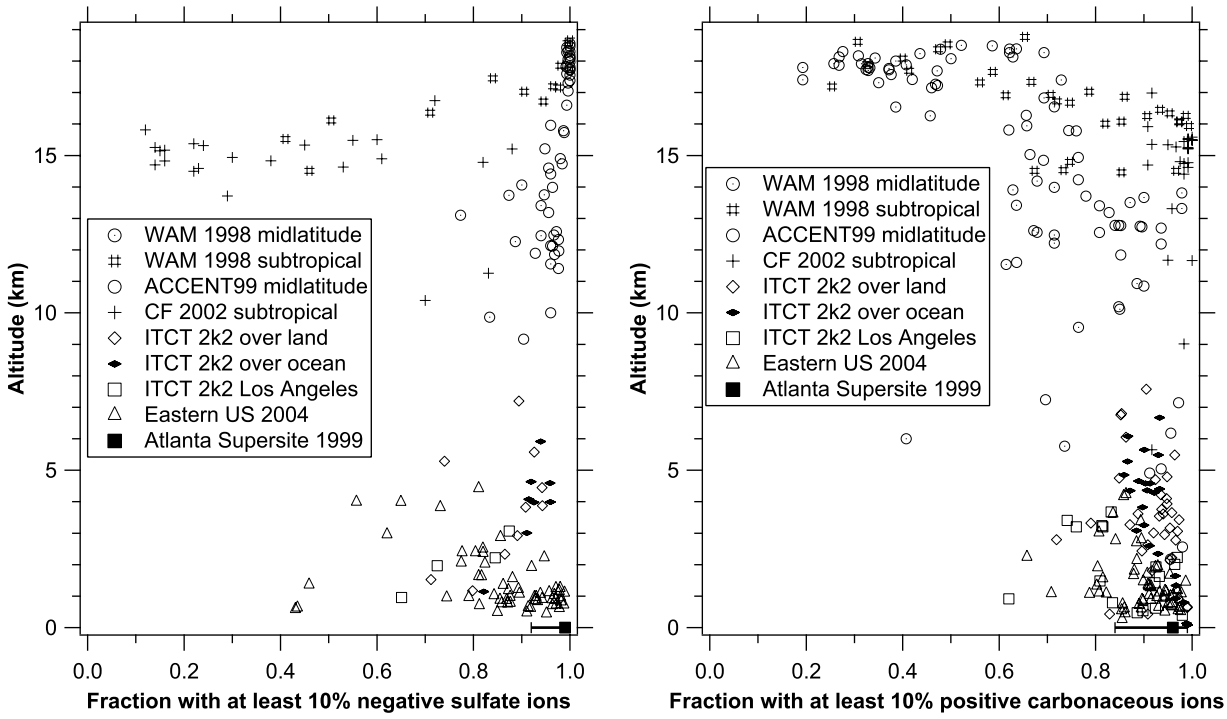

Figure 2. Fractions of single-particle mass spectra containing some sulfate in the negative ion mode or carbonaceous material in the positive ion mode. Each point is an average of 100 to 250 mass spectra at high altitudes and 1500 to 5000 mass spectra at low altitudes, except the Atlanta point is an average over the entire deployment with a bar showing the range of approximately half day averages.

fraction of a second at about 265 K. The capillary inlet undersampled small particles with an approximately diameter cubed size bias. The aerosol focusing inlet has much smaller biases and better overall particle transmission but does not transmit particles much larger than 3 μm diameter.

3. Carbonaceous-Sulfate Mixtures

[9] One of the salient features of the mass spectra is how many particles are internal mixtures of sulfates and carbonaceous material. Figure 1 shows some sample spectra of the most typical particles. The largest peak in many positive ion spectra is C^+ from the extensive fragmentation of organic and other carbonaceous molecules. The two examples show spectra with and without a large K^+ peak from biomass burning [*Hudson et al.*, 2004]. Although both particles clearly have the largest peaks from carbon species, the extensive fragmentation from the intense excimer laser pulse means that most information about the molecular species is lost. In such mixed particles, it is hard to tell if there is also elemental carbon present, since the peaks it produces (C^+, C_2^+, C_3^+, etc.) can also be made from organic molecules. Pure soot particles have a clear mass spectral signature but there are probably many more mass spectra where the peaks from elemental carbon are obscured by similar peaks from organic molecules. For example, in Figure 1 we are not able to determine the relative contributions of elemental carbon and organics to the C_2^+ peak.

[10] The negative ion spectra in Figure 1 both show mixtures of carbonaceous and sulfate compounds. The negative mass spectra are much less sensitive to organics, so the sulfate peaks are relatively much more pronounced. One negative ion spectrum (Figure 1c) is most representative, showing some carbonaceous peaks with little molecular information. The other spectrum (Figure 1d) shows a wider variety of organic and halogen ions. Some of the peaks such as HCO_2^-, the formate ion, probably represent fragments of larger molecules rather than formic acid in the particle. Still, the spectrum does show that there were oxygenated organics present. This spectrum is very typical of particles observed just below the tropopause, but can be found at lower altitudes as well.

[11] By looking at many mass spectra, it is clear that most particles are internally mixed, that is, they contain carbonaceous material and sulfates in the same particle. With varying amounts of sulfate and carbonaceous material in each particle, there is no simple definition of internal mixing. Particles can be internally mixed in the sense that each particle contains more than one chemical component yet be externally mixed in the sense that there are different types of particles in the same air. Figure 2 shows the fraction of particles with at least 10% of the ion current in either carbonaceous or sulfate peaks. In each case the polarity has been chosen to be more sensitive, so these criteria may represent as little as a few percent of carbonaceous material or sulfate in a given particle. Still, it is striking that most particles contain both. The particles without sulfate at about 15 km are from biomass burning plumes encountered in 2002 [*Jost et al.*, 2004] and a separate plume in 1998. Another fire plume is responsible for some of the low sulfate fractions at about 4 km. Essentially all particles above about 17.5 km contain sulfate. Except in the stratosphere, most particles contain detectable amounts of carbon compounds. The profile of carbonaceous material in particles in the stratosphere is discussed separately [*Murphy*

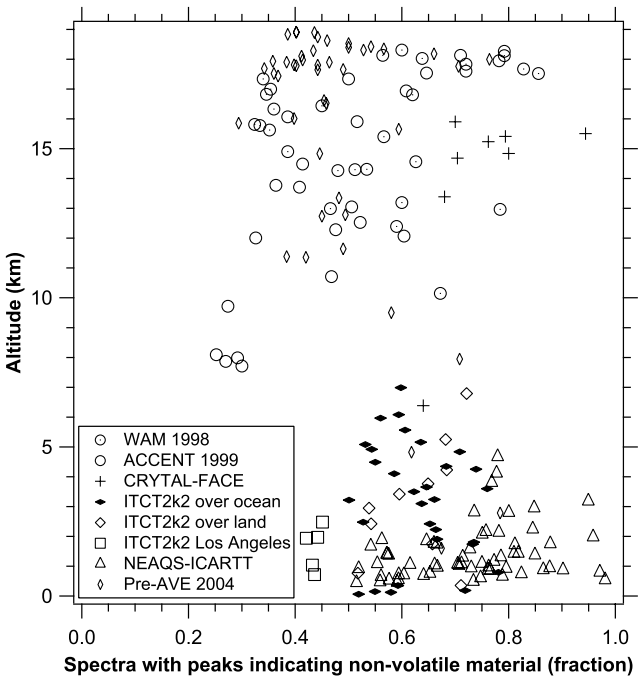

Figure 3. Fractions of positive ion mass spectra containing some peaks that indicate material that must have come from surface or extraterrestrial sources rather than condensation. The most common such peaks are potassium in the troposphere and iron in the stratosphere. Particles with lithium, sodium or patterns indicative of minerals or metals are also included. Each point is the frequency in 100 to 400 mass spectra at high altitudes and 1500 to 5000 mass spectra at low altitudes.

et al., 2006a]. The low-altitude data from the eastern US are consistent with our data from the Atlanta Supersite in 1999, where most particles contained both sulfate and carbonaceous material [*Lee et al.*, 2002].

[12] Even though these mixing results are not quantitative, they still have an important implication for modeling cloud formation. In order to model cloud formation, the water uptake near 100% relative humidity has to be described. For mixtures of comparable amounts of organic material and sulfate, the water uptake by individual can be approximated as a linear combination of the water uptakes of the sulfate and a less hygroscopic organic fraction [e.g., *Badger et al.*, 2005; *Garland et al.*, 2005; *McFiggans et al.*, 2005b]. This approximation breaks down for pure organic particles, which in principle display a different water uptake for every substance. At least for adipic acid, less than 10% sulfate is needed to come close to the simpler linear mixing approximation for water uptake [*Broekhuizen et al.*, 2004]. The PALMS data show that most of the particles in the troposphere probably have sufficient sulfate for this to be a good approximation. Actually, because it only considers sulfate, Figure 2 understates the number of particles that contain ionic material. For example, almost all of the 20 to 30% of particles in the Los Angeles basin that did not have measurable sulfate contained enough nitrate that they probably satisfied a linear approximation to water uptake by mixed organic-ionic particles. The degree of internal mixing is not so perfect that particle-to-particle variations in ionic and organic content are unimportant to cloud formation. Instead, it means that the extremes of pure sulfate or pure organic particles are uncommon, so that if a cloud model only considers one or two types of particles they should be internal mixtures.

[13] One other aspect of internal mixing is the frequency with which low-volatility elements are detected (Figure 3). At all altitudes, over half of the mass spectra usually contain peaks that indicate that the particles contain more than the sulfate, carbonaceous material, and other species that can condense out of the gas phase. Potassium, mostly from biomass burning, is the most common nonvolatile element. In the stratosphere meteoric metals are present in about half the particles in the PALMS size range. There are a wide variety of other minerals and metals as well. Probably even more particles contain nonvolatile material that does not show up well in the mass spectra. One example is elemental carbon, which is present in small amounts in many particles even in remote regions [*Posfai et al.*, 1999]. The presence of so many particles with nonvolatile material means either that a significant fraction of optically active particles are derived originally from surface and other sources apart from new particle formation, or that coagulation is fast enough to mix particle types.

[14] Figure 4 shows comparisons between the relative carbonaceous signal for PALMS versus AMS organic and PILS water-soluble organic carbon, each compared to sulfate. The quantities are not strictly comparable: there are different size biases in the instruments, notably the low sensitivity of PALMS to particles less than about 300 nm diameter and reduced sensitivity of the AMS to particles larger than about 600 nm diameter. The PILS instrument reports the atmospheric mass (μg m^{-3}) of soluble inorganic ions and water-soluble organic carbon (WSOC) particles. The AMS instrument reports the atmospheric mass of various species as derived from calibrations of the efficiency of volatilization and ionization. The AMS organic and sulfate mass determinations makes use of an approximate relationship between the mass of a molecule and its electron impact ionization cross section [*Jimenez et al.*, 2003]. The PALMS data give ion fractions. The carbonaceous negative ion fraction for PALMS is expected to underestimate the organic content because sulfates very readily make negative ions, particularly HSO_4^-. Thus it is expected that on Figure 4 most of the points lie below a 1:1 line. The greater linearity of the PALMS-PILS comparison may indicate simply that PALMS negative ions and water-soluble organic carbon both underestimate the organic content. However, there may be a more subtle reason: laboratory studies with PALMS have shown that glycerol produced negative ions more readily than tridecane. It may be that the negative ions in PALMS are responding preferentially to molecules also included in the PILS water-soluble measurement.

[15] In direct comparisons of PALMS and AMS data using laboratory-generated WSOC/sulfate particles, the relationship between the PALMS carbonaceous/(carbonaceous + sulfate) negative ions and AMS organic/(organic + sulfate) was similar to that shown in Figure 4. Furthermore, the AMS measured fraction was linear (r-squared of 0.95 and slope of 1.0 ± 0.1) compared to the actual fraction whereas the PALMS ion fraction had varying amounts of nonlinearity depending on the organic species. This is consistent with a varying and generally lower sensitivity to organics compared

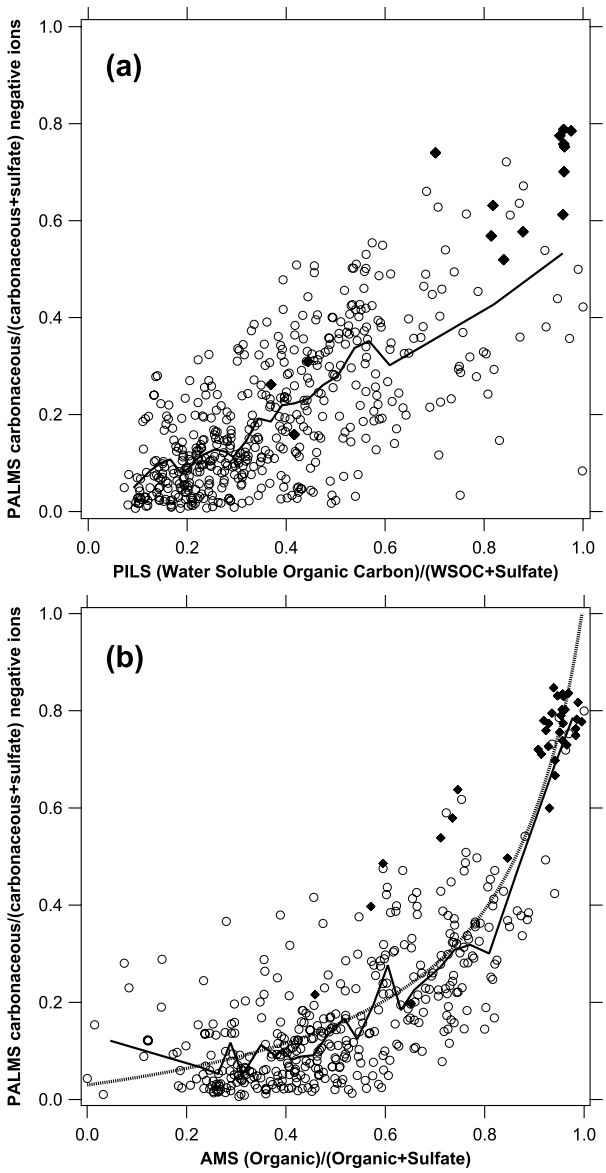

Figure 4. Comparisons of PALMS carbonaceous and sulfate ion fractions to (a) PILS and (b) AMS mass fractions during the 2004 P3 flights. Each point is an average of 300 mass spectra, or the spectra are averaged down to 25 bins (solid lines). Solid points are times when acetonitrile was greater than 300 ppb, indicating biomass burning influence. In an attempt to use comparable size cuts, PALMS mass spectra were not included for particles with aerodynamic diameters larger than 750 nm for the AMS comparison and 1 μm for the PILS comparison. Only times with organic plus sulfate loadings of greater than 1 μg m^{-3} for AMS or 0.5 μg m^{-3} for PILS were included. The dotted line in Figure 4b shows a smooth fit used in Figure 5.

to sulfate in the negative ion PALMS data. Much of the scatter in Figure 4 can be explained by the different responses of PALMS, PILS, and the AMS to different types of carbonaceous material. Using 5-min averages, the AMS organic mass and PILS WSOC data on the NOAA P3 in 2004 in air without a biomass burning influence were linearly correlated with an r-squared of 0.57 and a slope of 2.1 ± 0.8 μg μgC^{-1}. This was not nearly as good as the PILS and AMS sulfate correlation (r-squared of 0.80 and a slope of 1.0 ± 0.1).

[16] The comparisons of PALMS to AMS and PILS (Figure 4) can be used to approximately calibrate the vertical profiles shown in Figure 5. The fit shown in Figure 4b is consistent with PALMS being about 7 times as sensitive to sulfate as organics in the negative ion mode with a small intercept because of carbonaceous material measured by PALMS but not the AMS. A benefit of this approach is that it uses organics in the atmosphere rather than idealized laboratory particles. Figure 5b shows the ion ratios transformed using the fit shown on Figure 4. PALMS has taken data at higher altitudes and at particle concentrations that would be below the detection limit of the AMS. The PALMS carbonaceous/(carbonaceous + sulfate) negative ion ratios in the upper troposphere of 0.2 to 0.4 suggest carbonaceous mass fractions in the upper troposphere of 0.3 to 0.8, with a wider range below 5 km. Approximately the same mass fractions can be obtained by fitting the PALMS ion ratios to the PILS water-soluble organic carbon multiplied by 1.5 to 2 to account for insoluble organics in the free troposphere [*Putaud et al.*, 2004]. The Atlanta Supersite data also support a high organic fraction in the upper troposphere. Sulfate and organic mass fractions were similar to each other in Atlanta [*Baumann et al.*, 2003], yet the PALMS carbonaceous negative ion fractions in the upper troposphere were often larger than the mean PALMS value in Atlanta.

[17] Even though PALMS cannot completely distinguish organic and elemental carbon, several lines of evidence support the idea that most of the carbonaceous mass in the upper troposphere is organic. First, the PALMS carbon peaks are correlated with both AMS and PILS. Such a correlation would not be expected if PALMS had been measuring primarily elemental carbon to which the AMS and PILS are not sensitive. Second, electron microscope analyses by *Sheridan et al.* [1994] at similar latitudes to our data found that fewer than 1% of the particles in the upper troposphere were soot. We also found that pure elemental carbon particles were rare. Although *Posfai et al.* [1999] found soot inclusions in many particles in the remote free troposphere, it is also clear in their data that these inclusions were not a large fraction of the mass. Third, a large mass fraction of elemental carbon in the upper troposphere would be inconsistent with measurements of the nonvolatile fraction of particles there [*Clarke*, 1993]. *Novakov et al.* [1997] estimated that 10% of the carbon mass in the free troposphere was black carbon.

[18] Figure 6 shows the distribution of the PALMS carbonaceous/(carbonaceous + sulfate) negative ion ratio with altitude and latitude. The stratosphere stands out as a region of nearly pure sulfate particles. Otherwise, there is no simple pattern, a consequence of the lifetime of aerosols in the troposphere being short enough that their properties are not smoothed out over North America. In the boundary layer at 40°N, one can find anything from nearly pure organics to pure sulfates depending on time and location [*Brock et al.*, 2004]. The significant amount of carbonaceous material throughout most of the free troposphere is consistent with *Novakov et al.* [1997].

[19] Figure 7 shows the average carbonaceous/(carbonaceous + sulfate) negative ion ratio as a function of vacuum aerodynamic diameter (proportional to diameter times density). The graph does not extend to the smallest particles

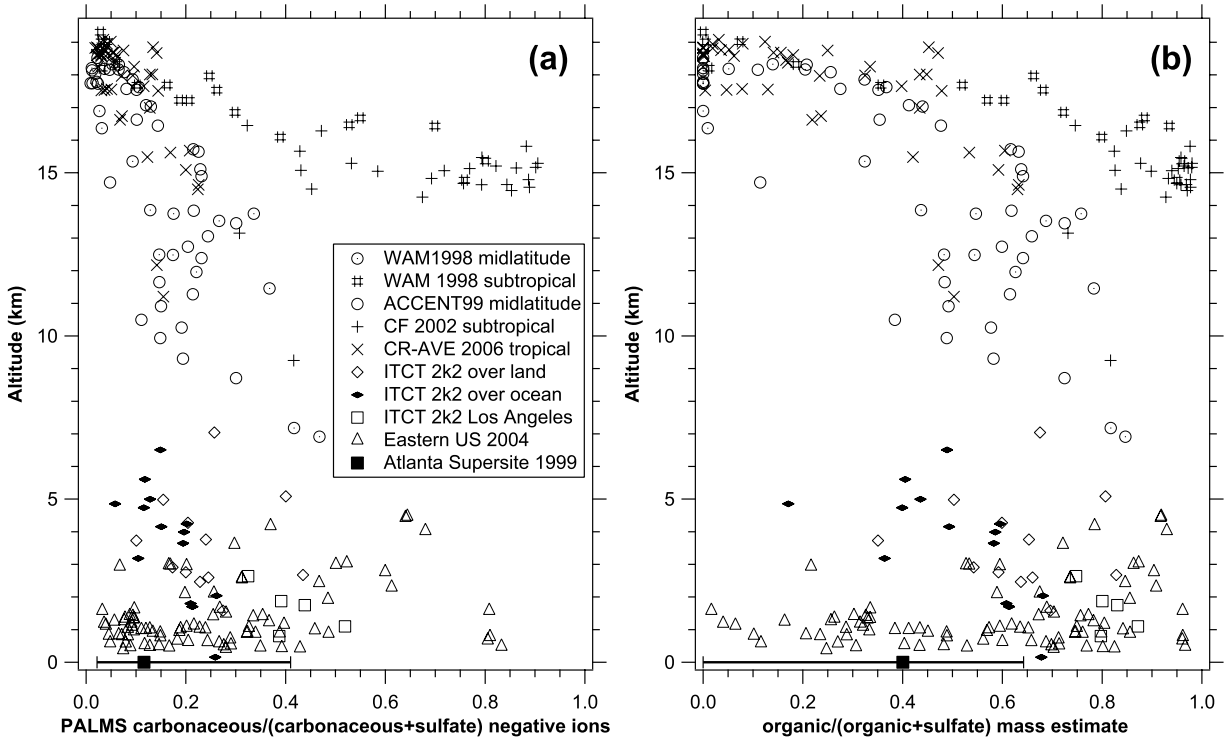

Figure 5. (a) Vertical profile of the fraction of carbonaceous ions based on negative ion mass spectra. Although many peaks were considered, the peaks contributing the most carbonaceous ion signal were C^-, C_2^-, C_2H^-, and CN^-. The most important sulfate peak was HSO_4^-. Each point is an average of 100 to 250 mass spectra at high altitudes and 1500 to 5000 mass spectra at low altitudes, except the Atlanta point is an average over the entire deployment with a bar showing the range of approximately half day averages. (b) Ion ratios transformed to approximate mass fraction using the fit of the PALMS to the AMS data shown in Figure 4b. Mass fractions below about 0.3 are especially uncertain because the negative ion mass spectra are not well suited to small organic fractions, and the fit in Figure 4b is nearly horizontal at small mass fractions, implying great uncertainty when it is inverted.

measured by PALMS because of composition biases there. At a given aerodynamic diameter, a high-density particle will have a smaller geometric diameter and may not be detected as easily by the continuous laser. Even allowing for this effect, it appears that the smallest particles have larger carbonaceous content, as observed at ground and mountain sites [*McFiggans et al.*, 2005a]. Sea salt and dust are excluded from the figure, an important consideration when interpreting the data above 1 μm, where the higher carbonaceous content near the ground may indicate a primary source of carbonaceous particles.

4. Nitrate

[20] Nitrate was much less common than sulfate. In our airborne data to date, the only low-altitude locations with nitrate consistently exceeding sulfate were certain parts of the boundary layer over southern California [*Neuman et al.*, 2003]. Nitrate is predicted to become more important relative to sulfate in the future because of relatively lower sulfate emissions [*Liao and Seinfeld*, 2005]. The basic thermodynamic prediction at temperatures above about 200 K is that nitrate is stable on sulfate particles only when they are fully neutralized [*Bassett and Seinfeld*, 1984]. The PALMS data on nitrate are in accord with this prediction. Nitrate was almost always present in one of three conditions: mixed with sulfate

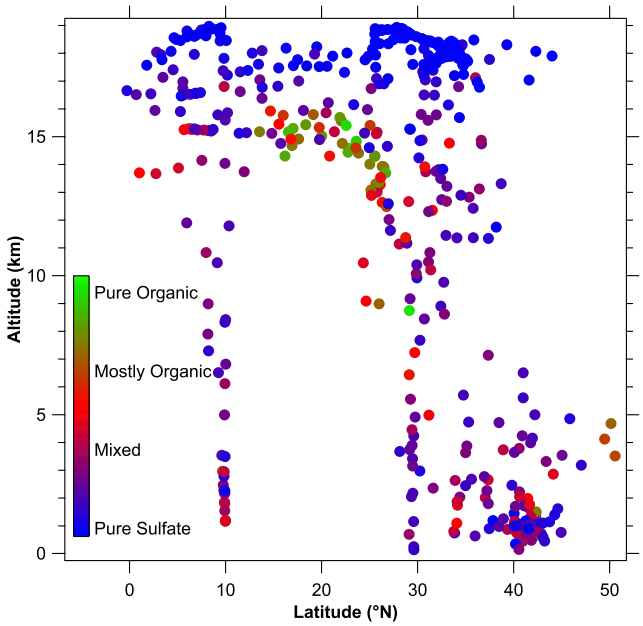

Figure 6. An altitude-latitude cross section of the fraction of carbonaceous ions based on negative ion mass spectra, as shown in Figure 5.

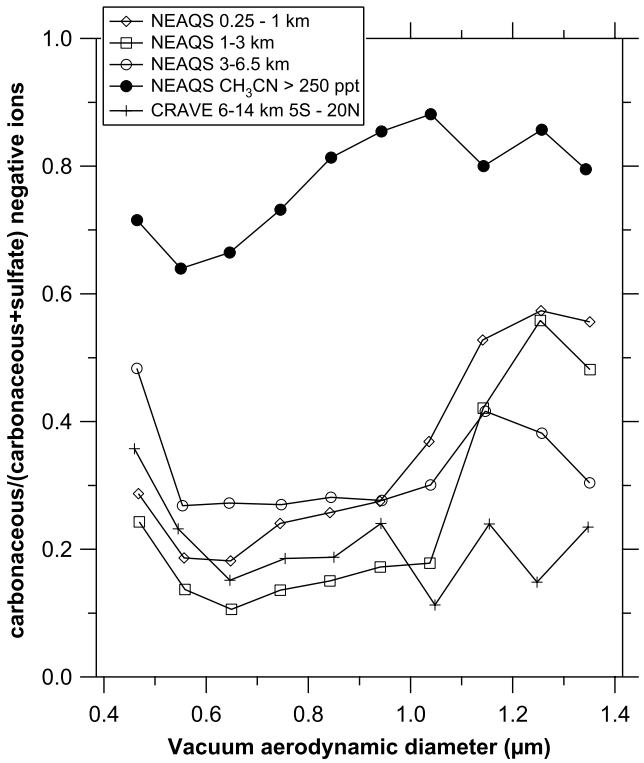

Figure 7. Fraction of carbonaceous ions in negative ion mass spectra of mixed carbonaceous-sulfate particles as a function of vacuum aerodynamic diameter. The three NEAQS altitude ranges are from periods with acetonitrile less than 160 pptv.

and carbonaceous material in areas where the aerosol was fully neutralized, on mineral particles where cations other than ammonium can stabilize the nitrate, or near a cold tropopause. Nitric acid has also been detected on ice crystals near the tropopause [*Popp et al.*, 2004; *Ziereis et al.*, 2004]. Nitrate can also replace the chloride on sea salt [*Gard et al.*, 1998], but since very few sea salt particles are found in the free troposphere this form of nitrate was less important for the aircraft data described here.

[21] The choice of nitrate peaks in the mass spectra is complicated. Negative ion masses 46 and 62 are almost always due to NO_2^- and NO_3^-. These peaks seem to be due only to nitrates. However, NO_2^- and NO_3^- are not ideal because they tend to be very small peaks. Nitrates also produce O^- but that peak is not unique to nitrate.

[22] A prominent peak in the positive ion spectra is often NO^+. Using another single-particle mass spectrometer (ATOFMS), NO^+ was identified as originating from nitrate [*Pastor et al.*, 2003] by comparison to impactor (MOUDI) measurements of nitrate. In our case, although NO_2^- and NO_3^- were correlated with PILS and AMS nitrate, the NO^+ peak was not well correlated. There are two possible explanations for the difference between our results and Pastor et al. First, the ionization is somewhat different. PALMS uses about a factor of ten higher laser intensity than ATOFMS as well as a shorter wavelength ionization laser (193 versus 266 nm). This could lead to more fragmentation and rearrangement. Second, it seems likely that NO^+ is indeed formed from nitrate but also can be formed with lower efficiency from ammonium and possibly other nitrogen containing molecules. PALMS laboratory spectra of $(NH_4)_2SO_4$ particles have a large NO^+ peak. *Pastor et al.* [2003] sampled an environment rich in ammonium nitrate where a contribution to NO^+ from ammonium would reinforce rather than destroy the correlation with nitrate. In the free troposphere with only occasional nitrate, even a small contribution from ammonium would obscure the relationship of NO^+ to nitrate.

[23] Despite the issues in choosing the best peaks to represent nitrate, there are clear patterns in the mass spectra. Figure 8 shows the relative size of the NO_2^- and NO_3^- in single particles as a function of the bulk ammonium to sulfate ratio measured by PILS. The data are separated into mineral particles (Figure 8, top) and mostly carbonaceous-sulfate particles (Figure 8, bottom). Nitrate was present on mineral particles regardless of the overall acid balance of the bulk aerosol. On the other hand, when nitrate was found on carbonaceous-sulfate particles, it was almost always when the sulfate was fully neutralized. Of the few nonmineral particles that contained nitrate when the sulfate was not neutralized, many either had peaks indicative of phosphorus (PO_2^- and PO_3^-) or elemental carbon. Of the remainder, there is the possibility that our use of silicon as a criterion to exclude mineral particles may have let through a few particles with, for example, calcium nitrate but no silicon.

[24] The third region where we have found nitrate on particles is at the tropopause, where there was uptake of nitric acid onto particles when the ambient temperature was below about 198 K [*Murphy and Thomson*, 2000] (aircraft

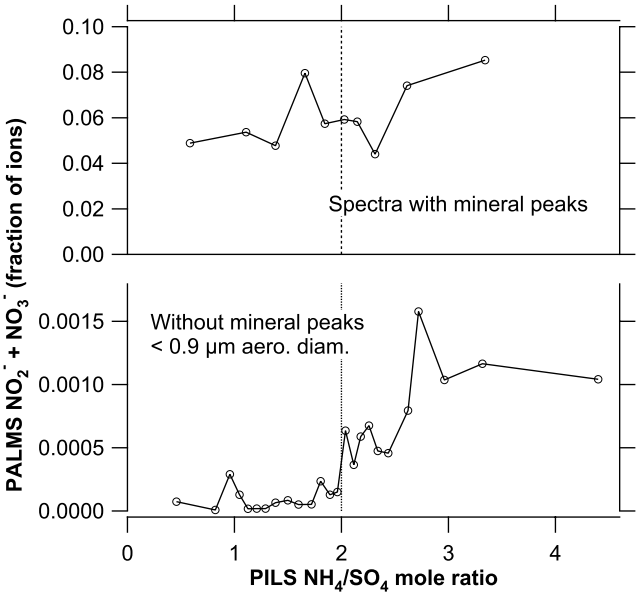

Figure 8. Fraction of ion current in the two most important negative ion nitrate peaks. The spectra have been sorted to be out of clouds (relative humidity less than 93%), have signal to noise greater than about 50, and be out of strong biomass burning plumes (acetonitrile less than 250 ppb). Mass spectra with mineral peaks have about 50 times the nitrate signal of particles without mineral peaks, and they continue to contain nitrate when the sulfate is not fully neutralized. Each point with mineral peaks is an average of 200 spectra, and each point without mineral peaks is an average of 4000 spectra.

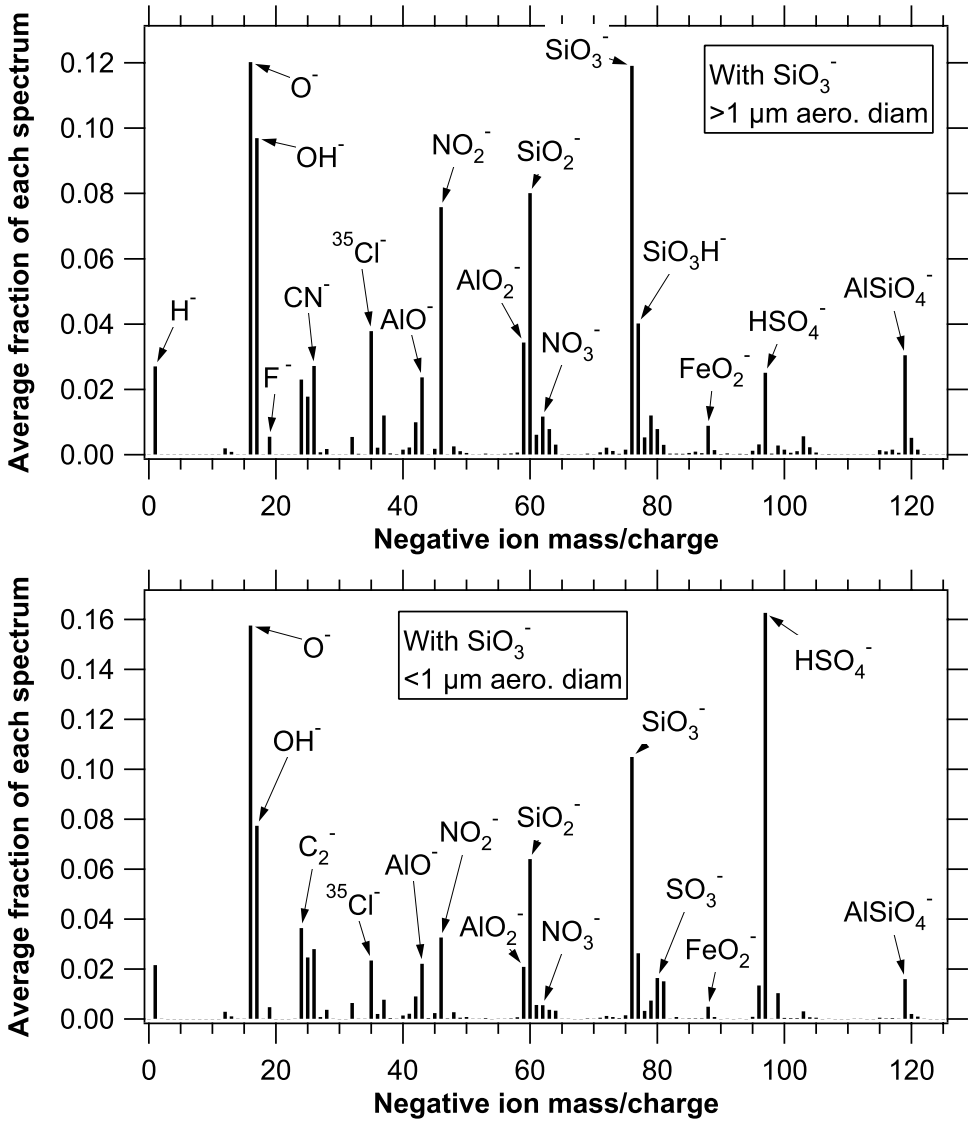

Figure 9. Average negative ion mass spectra of silicon-containing particles during the 2004 NEAQS experiment. Nitrate and/or chlorine peaks were present in the majority of such mass spectra.

temperature data have been updated to change the threshold from the 195 K stated in that paper). The nitric acid is volatile enough that it could only be measured using the capillary inlet with the very short residence time.

5. Mineral and Salt Particles

[25] In our first field measurements at a mountain site in Colorado, we found that coarse mode mineral particles often contained nitrate [*Murphy and Thomson*, 1997]. Indeed, in flow conditions that excluded local pollution, sorting the database for mass spectra with silicon peaks or for spectra with nitrate peaks yielded much the same sets of particles. The partitioning of nitric acid between particles and the gas phase means that nitrate can migrate from acidic particles to ones where the nitrate can be stabilized as calcium nitrate or other species. In contrast, there was much less sulfate in the mineral particles. Once sulfate is on a particle, it cannot easily migrate, so it stays on the accumulation mode particles with most of the total surface area. The airborne data continue this pattern.

[26] Mineral particles show up both in the positive ion spectra (Al^+, Ca^+, Fe^+, etc.) and the negative ion spectra (SiO_2^-, SiO_3^-, AlO^-, etc.). The negative ion silicon peaks are more unique to mineral dust than the positive ions, for which there are often either other ions at the same mass (e.g., ^{28}Si and CO^+) or other sources (e.g., Na in both mineral dust and sea salt). Therefore we use SiO_3^- as an indicator of mineral particles. By this criterion, both dust and fly ash are probably counted as mineral. For the 2004 NEAQS data set above 200 m (this excludes final approaches to airports and the very lowest altitude data over the ocean) there were 369 negative ion spectra smaller than 1 μm aerodynamic diameter and 779 larger than 1 μm that had a SiO_3^- peak of at least 1% of the total ion current. Because of size biases in the PALMS inlet, it is not valid to compare the absolute numbers of mineral particles below and above 1 μm. However, the size biases should be similar for mineral and nonmineral particles so it is

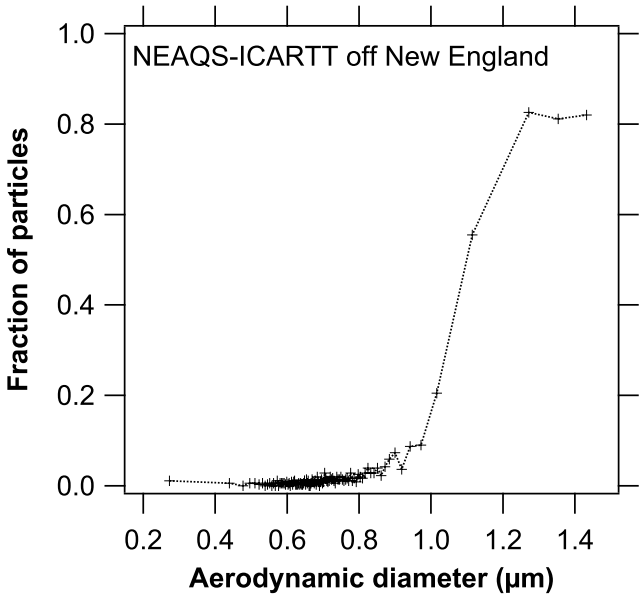

Figure 10. Fraction of sea salt particles in the marine boundary layer near New England. These are 400 particle averages of all mass spectra over the ocean, below 1 km, out of cloud, and with a dew point greater than 12.5°C. The PALMS inlet runs in a pressure range where the conversion of aerodynamic to geometric diameter goes as approximately the density to the first power, so the transition point is much smaller than 1 μm in geometric diameter.

relevant that 9% of particles larger than 1 μm produced a SiO_3^- peak whereas fewer than 0.2% of those smaller than 1 μm produced that peak. Figure 9 shows average mass spectra of particles with a SiO_3^- peak. Most notable are the large NO_2^-, HSO_4^-, and Cl^- peaks in the average mineral spectra.

[27] Of the particles with silicon, 61% of those smaller than 1 μm and 78% of those larger than 1 μm also had measurable NO_2^- or NO_3^- peaks from nitrate. In contrast, of particles without SiO_3^- only 6% and 39% smaller or larger than 1 μm had NO_2^- or NO_3^- (n = 234873 and 7505 respectively). Chlorine was also common in the mass spectra of mineral particles: 54% of those smaller than 1 μm and 74% of those larger than 1 μm contained chlorine. There was probably less chloride than nitrate on the mineral particles because not only are the average chlorine peaks smaller but also in negative ion mode PALMS is likely more sensitive to chloride than nitrate. The mass spectra of smaller mineral particles show more sulfate than those of larger particles, which is consistent with the relative amount of sulfate being determined by the surface to volume ratio.

[28] The uptake of nitrate by mineral particles has been measured many times, including single-particle electron microscope data that are more quantitative than the mass spectra presented here. Scavenging of nitrate by dust is important in Asian outflow [*Y. N. Lee et al.*, 2003; *Kline et al.*, 2004]. The significance of the mass spectra here is how widespread the association between mineral particles and nitrate was over the northeastern United States as well as earlier measurements in Colorado.

[29] The association of chloride with mineral particles has been noted less frequently. *Li and Winchester* [1993] inferred scavenging of chloride by dust particles in the Arctic. *Faude and Goschnick* [1997] measured chlorides at the surface of dust particles. *Aymoz et al.* [2004] measured more chloride in a Saharan dust plume than expected for halite minerals. *Zhang and Iwasaka* [2001] measured chlorine on dust particles in Japan. The amount of chloride was nearly as much as sulfate, and single-particle electron microscopy showed that much of the chlorine had been deposited from the gas phase rather than coming from coagulation with sea salt particles. Scavenging of chlorine from the gas phase by minerals is often thermodynamically favorable [*Kelly and Wexler*, 2005].

[30] The PALMS data are consistent with deposition of chloride from the gas phase. First, the chlorine was present as small peaks in many mass spectra, an indicator of uptake from the gas phase. Second, there was often chloride on mineral particles without peaks characteristic of sea salt or other chloride-containing particles that might have coagulated with the mineral particles. Most of the mineral particles described here were measured over the continental United States, where coagulation with sea salt is not expected to be important. Although internally mixed mineral and sea salt particles were found in air that had spent days in the tropical marine boundary layer [*Andreae et al.*, 1986], they were rare in the free troposphere over Japan [*Trochkine et al.*, 2003].

[31] Almost all sea salt particles were observed near the ocean surface. Far fewer than 1% of the particles measured in the free troposphere were sea salt. Figure 10 shows the fraction of particles that were classified as sea salt as a function of diameter for low-altitude airborne data off New England. This is a very different pattern than observed at Cape Grim, Tasmania, where mass spectrometer, electron microscope, and thermal volatility measurements all suggested that essentially all particles larger than about 120 nm contained sea salt [*Murphy et al.*, 1998b]. Less pollution, higher wind speeds, and a longer fetch over the ocean all contribute to a higher fraction of sea salt aerosols at a given size. Aerodynamic sizing was not used in the 2002 measurements off the California coast, but the optical sizes derived from the light scattered by each particle suggest that region was intermediate: the accumulation mode appeared to be an external mixture of modified sea salt and carbonaceous-sulfate particles.

6. Other Mass Spectral Patterns

[32] The mass spectra contain a rich amount of information on the particle composition. Some of the better understood patterns have already been published: halogen ions in the marine boundary layer and near the tropopause [*Murphy et al.*, 1997; *Murphy and Thomson*, 2000], biomass burning signatures [*Hudson et al.*, 2004], meteoric metals [*Murphy et al.*, 1998a], and mercury [*Murphy et al.*, 1998a, 2006b]. A few other special peaks are presented here.

[33] CN^- is an important peak but its interpretation is not clear. It was often the largest negative organic ion and was even the largest peak in many negative ion spectra. There is some contribution to mass 26 from $C_2H_2^-$, but the relative size of 26 to 25 (C_2H^-) makes it clear that the majority of the ion current at mass 26 is CN^-. When the CN^- peak is large, its

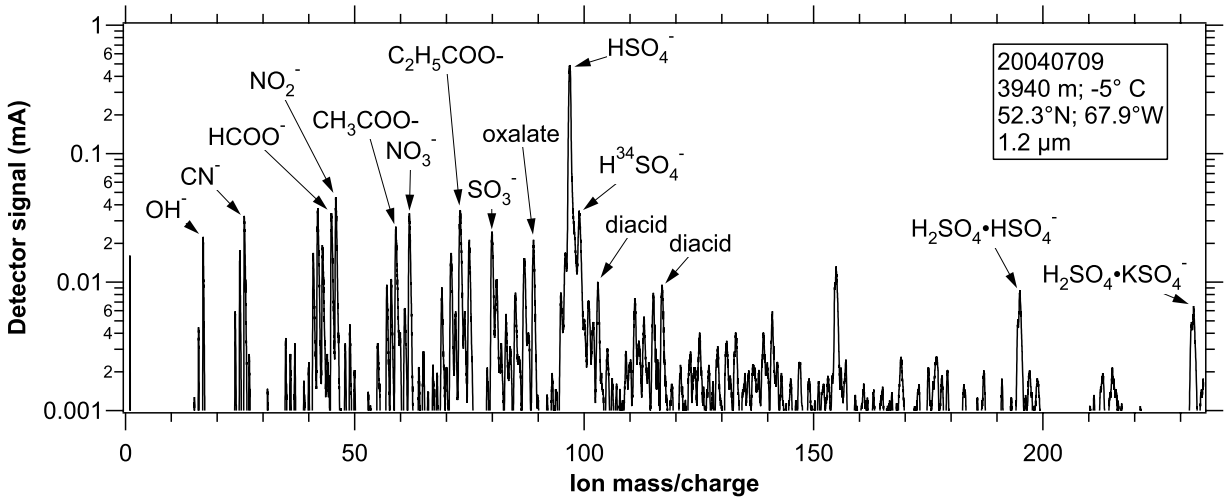

Figure 11. An example of a negative ion mass spectrum showing mixed sulfate and organic acid fragments. The small signals are a large number of small organic peaks, not noise.

identity can be confirmed with mass 27 from the ^{13}C and ^{15}N isotopes. There was also often a peak at mass 42 that is probably CNO^-. The nitrogen cannot be coming from residual air in the ion source because there is no CN^- peak in the laboratory mass spectra of a variety of organic particles that do not contain nitrogen. The question is whether the CN^- indicates that there were carbon-nitrogen bonds in the organic molecules. Limited laboratory data suggest that CN bonds can be formed during the laser ionization, but some of the CN^- may come from amides, amines, or other forms of organic nitrogen in the particles [*Milne and Zika*, 1993; *Angelino et al.*, 2001; *Cornell et al.*, 2003].

[34] One of the more common patterns negative ion organic peaks was a set of organic acid fragments in addition to or often in place of the small fragments shown in Figure 1. About 10% of negative ion mass spectra between 5 and 15 km contained organic acid peaks. The pattern was less frequent at low altitudes, but was still present in ground-based data in Atlanta, where the organic acid peaks were largest between 6 and 10 am local time [*S. Lee et al.*, 2003]. A sample of this organic pattern from the midtroposphere is shown in Figure 11. The formate, acetate, and some further acid peaks are most likely fragments of larger acids. The ions indicative of the potassium salts of sulfuric and probably succinic acid were common but not universal in such spectra.

[35] As in Figure 11, mass spectra with organic acid peaks typically had a very large sulfate peak. Both sulfate and organic acids can be formed by liquid phase chemistry in clouds [*Ervens et al.*, 2004]. Although at 1.2 μm this particular particle was larger than most, such spectra were on average slightly larger than other carbonaceous-sulfate particles measured by PALMS, which is also consistent with cloud processing. Spectra rich in organic acids were found in a slightly higher fraction of particles within biomass burning plumes than outside them. Their nitrate content was similar to other particles. With large sulfate peaks and similar nitrate peaks, spectra with organic acids had to have relatively less of something else. That decrease was in the small organic fragments such as C_2^- and CN^-.

[36] The various organic acid negative ions (monoacids at 45, 59, etc; diacids at 89, 103, 117, etc.; 155 probably $KOOCC_2H_2COO^-$) all had similar vertical profiles with

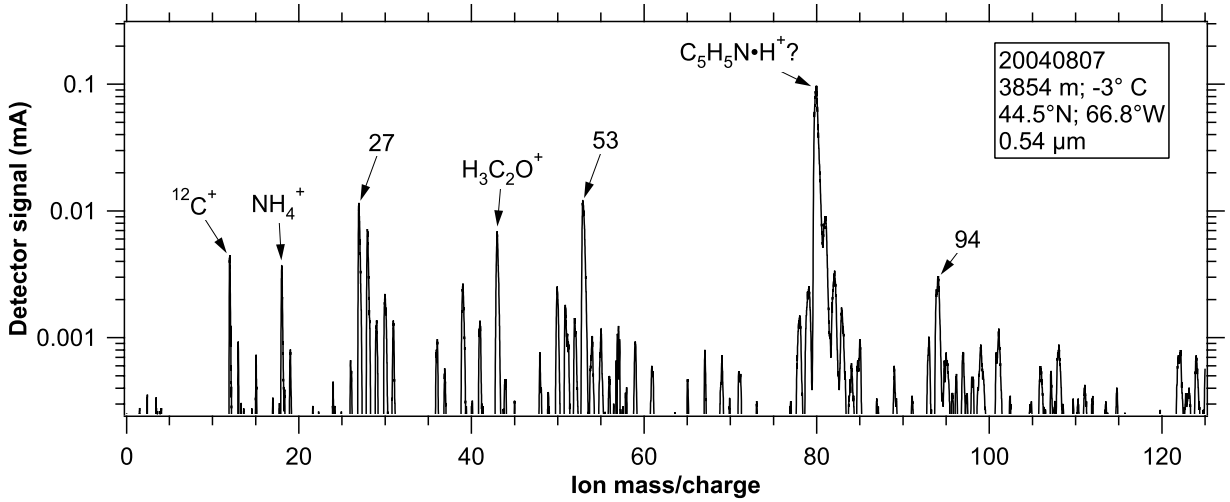

Figure 12. An example of a positive ion mass spectrum showing probable pyridine.

broad maxima in the free troposphere. They formed a 2 to 5 times higher fraction of the ions at 4 to 10 km than in the boundary layer. Their abundance fell off again in the stratosphere. No fine structure within the troposphere could be discerned because different altitudes were sampled in different regions and indeed from different aircraft. Only the decreases at the top and bottom of the vertical profile were robust over all the missions. Oxalic acid has a special importance since it can heterogeneously nucleate ice [*Zobrist et al.*, 2006].

[37] A fairly unusual but interesting peak in the mass spectra is an isolated positive ion peak at mass 80, sometimes accompanied by a peak at mass 94 (Figure 12). Such spectra were very rare in the stratosphere and below 1 km. They reached a maximum of about 1% of the particles at about 10 km during the ACCENT mission. In the 2004 NEAQS data (for which aerodynamic diameters are available) many of these particles were larger than 1 μm. In these spectra mass 80 cannot be SO_3^+ because the mass 82 peak is too small for the ^{34}S isotope. A tentative assignment is protonated pyridine. Pyridine has a high proton affinity and protonated pyridine is the most abundant positive core ion in the free troposphere [*Eisele*, 1988; *Schulte and Arnold*, 1990]. Figure 12 also shows prominent peaks at masses 27 and 53, which are the most abundant fragment ions from MS-MS of protonated pyridine [*Eisele*, 1988].

[38] Even though the extrapolated vapor pressure of pyridine is far too high for simple condensation [*Chirico et al.*, 1996], it is not too surprising that pyridine can partition to aerosols at cold temperatures, especially if the particles contain organics. What is more surprising is that there could be enough pyridine in a particle for it to be the largest peak in the mass spectrum. One possibility is that the semivolatile pyridine migrates between particles until it has high concentrations in certain favorable particles. Another possibility is that the spectra with protonated pyridine as the largest peak were from particles where the combination of laser power, particle composition, and particle size led to more ion-neutral reactions during the laser ablation and ionization. Then the very high proton affinity of pyridine could allow it to be the most abundant positive ion even if it were not the most abundant constituent of the particle. Still, there would have to be enough pyridine in the particle to make that many positive ions.

[39] Some order of magnitude calculations support enough pyridine to account for the isolated mass 80 peak. *Schulte and Arnold* [1990] estimated a gas phase pyridine abundance of 1.6 pptv and *Tanner and Eisele* [1991] estimated 2.5 pptv. That is roughly 0.3% of a total particle mass loading of 1 μg m^{-3} at standard conditions. If 1% of the particles contained 5% pyridine the amount would be less than the gas phase concentration. At a mixing ratio of 2 pptv, pyridine can add 0.1% mass to a 1 μm particle in as little as an hour, so there is plenty of time for some gas-particle partitioning to take place even though equilibration between particles is very slow at part per trillion gas concentrations. The pyridine was clearly not coming directly from anthropogenic sources since such mass spectra were rare when gas phase benzene was larger than about 60 pptv.

[40] A final comment on patterns in the mass spectra is that this overview naturally concentrates on a limited number of patterns in the mass spectra. One measure of this is that cluster analysis techniques normally can put over 99% of the mass spectra into about 20 clusters, and even some of these are not distinct types (i.e., separate clusters for carbonaceous material with sulfate versus sulfate with carbonaceous material). However, with over a million mass spectra, we have hundreds of mass spectra of very unusual particles. There is an astonishing variety to these. Except for the less common rare earth elements and the noble gases, almost every element has been measured in a least a few mass spectra. This includes some heavy metals such as thallium, uranium, and thorium. It is not really surprising that a sensitive analytical technique will see unusual results given a sufficiently large sample size. The presence of rare particles is not significant for mass budgets, direct radiative forcing, or global aerosol modeling. The most plausible atmospheric importance for rare particles is probably ice nucleation, which can occur on fewer than one in a thousand particles. Another significance for rare particles is the interpretation of other analytical techniques as they are pushed to low detection limits. For example, at the one in a thousand level, an optical particle counter sampling ambient air might encounter not only transparent and absorbing particles but also metallic particles with possibly unusual optical properties.

7. Discussion and Conclusions

[41] *Bates et al.* [2006] proposed a minimum set of types of particles that are sufficient to describe optical properties observed in several recent field experiments. These types are submicrometer carbonaceous-sulfate mixtures, submicrometer and supermicrometer mineral particles, and supermicrometer sea salt. The PALMS results are quite consistent with this set. A submicrometer sea salt mode might also be needed in areas not downwind of continents. On the other hand, the high degree of internal mixing of carbonaceous material and sulfate is not consistent with global aerosol models that carry carbonaceous material and sulfates separately. Whether or not this matters depends on the details of the treatment of aerosol properties. For nonabsorbing particles, the overall aerosol optical depth is not very sensitive to the degree of internal or external mixing [*Quinn et al.*, 2005; *Baynard et al.*, 2006]. A full treatment of cloud nucleation would be sensitive to the degree of mixing, but many global models use empirical correlations that presumably include the impact of whatever internal mixing was present in the field data used to generate the empirical correlations. As cloud formation in global models moves to more physically based parameterizations the models will have to do a better job of simulating the internal mixing of carbonaceous material and sulfates.

[42] The high degree of internal mixing of carbonaceous material and sulfates is consistent with tandem differential mobility analysis of water uptake of particles. Outside of urban areas, such analyses have often identified more than one hygroscopic mode, but a summary of the data in remote areas shows that multiple modes are present only a minority of the time, and even when present a hygrophobic mode is a small minority of the particles [*McFiggans et al.*, 2005b]. An important subtlety is that the spread of hygroscopicity within a single mode can still be important for cloud formation [*McFiggans et al.*, 2005b], so the PALMS data do not mean that all particles are alike for cloud formation.

[43] With the high degree of internal mixing between carbonaceous material and sulfates, one might expect that clouds would scavenge them with similar efficiency. The limited observations show cases of both similar and different cloud activation or scavenging efficiencies for carbonaceous material and sulfate. Nearly complete activation of particles larger than 200 nm was observed at Jungfraujoch, independent of particle composition [*Baltensperger et al.*, 1998]. In contrast, at Puy de Dome, *Sellegri et al.* [2003] found much higher scavenging efficiencies for inorganic ions in the accumulation mode (76–93%) than for organic species (14%). Elemental carbon was scavenged with intermediate efficiency (33–74%). In other studies, water-soluble organics were found to be scavenged with higher efficiency than insoluble organics [*Facchini et al.*, 1999; *Limbeck and Puxbaum*, 2000]. There are several possible ways to resolve internal mixing and differential scavenging. Unfortunately, without better data the explanations are only speculation. There is of course the possibility that the particles were different at those sites than at the locations observed by PALMS. Puy de Dome has a rather high fraction of water insoluble carbon [*Sellegri et al.*, 2003]. Also, PALMS observes the presence of carbonaceous material with sulfate in the same particles but seldom identifies the type of organics. There might be different populations of carbonaceous particles with different water solubility, perhaps driven by polar semivolatile organics being better solvated in particles with polar organics and vice versa. The tandem differential mobility hygroscopic analyses do not support this as being a common occurrence, however. Finally, the kinetics of cloud activation might make scavenging sensitive to small changes in composition, such as surface-active compounds, that PALMS does not readily differentiate from other carbonaceous material.

[44] Carbonaceous-sulfate mixtures are the dominant type of 200 to 1000 nm particles in the atmosphere in the free troposphere in all locations studied so far. Although the proportions of carbonaceous material and sulfate vary considerably, most particles contain at least some of both. Some of these mixed particles are attributable to condensation on nonvolatile cores such as meteoric material and potassium from biomass burning. Others contain nothing else observable except carbonaceous material, sulfates, and nitrates. Mineral dust and sea salt are the major other types of observed particles. These undergo important uptake of nitrate, chloride, and other species. Beyond those, there is a wide range of rare particle types. If the carbonaceous material includes organics at the surface of the particles, then heterogeneous chemistry of the particles may be significantly different than for pure sulfate particles [e.g., *Brown et al.*, 2006].

[45] One of the key outstanding questions is the degree of internal and external mixing of black carbon and other light absorbing material. The nature of light absorption in small particles means that the total amount of light absorbed is sensitive to this mixing [*Martins et al.*, 1998]. Other instruments will be needed to distinguish light absorption at the single-particle level.

[46] Another outstanding issue is the reason for the large carbonaceous fraction in the free troposphere. Sulfate is produced in the free troposphere starting from the oxidation of SO_2 by OH. All else being equal, the carbonaceous fraction would decrease with altitude. Lofted biomass burning plumes may contribute to the carbonaceous material but cannot be the only explanation because the majority of carbonaceous-sulfate particles in the upper troposphere did not contain potassium. One possible explanation is formation of secondary organic particulate matter in the free troposphere [*Heald et al.*, 2005]. Slower scavenging of carbonaceous material compared to sulfate by both liquid and ice [*Cziczo et al.*, 2004] clouds could also help maintain a large carbonaceous fraction.

[47] **Acknowledgments.** Joost deGouw and Carsten Warneke provided the acetonitrile data used for sorting Figure 4 by the influence of biomass burning. Tahllee Baynard and Roya Bahreini helped obtain and analyze the laboratory PALMS and AMS calibration data.

References

Andreae, M. O., R. J. Charlson, F. Bruynseels, J. Storms, R. Van Grieken, and W. Maenhaut (1986), Internal mixture of sea salt, silicates, and excess sulphate in marine aerosols, *Science*, *232*, 1620–1623.

Angelino, S., D. T. Suess, and K. A. Prather (2001), Formation of aerosol particles from reactions of secondary and tertiary alkylamines: Characterization by aerosol time-of-flight mass spectrometry, *Environ. Sci. Technol.*, *35*, 3130–3138.

Aymoz, G., J.-L. Jaffrezo, V. Jacob, A. Colomb, and C. George (2004), Evolution of organic and inorganic components of aerosol during a Saharan dust episode observed in the French Alps, *Atmos. Chem. Phys.*, *4*, 2499–2512.

Badger, C. L., I. George, P. T. Griffiths, C. F. Braban, R. A. Cox, and J. P. D. Abbatt (2005), Phase transitions and hygroscopic growth of aerosol particles containing humic acid and mixtures of humic acid and ammonium sulphate, *Atmos. Chem. Phys. Disc.*, *5*, 9581–9620.

Bahreini, R., J. L. Jimenez, J. Wang, R. C. Flagan, J. H. Seinfeld, J. T. Jayne, and D. R. Worsnop (2003), Aircraft-based aerosol size and composition measurements during ACE-Asia using an Aerodyne aerosol mass spectrometer, *J. Geophys. Res.*, *108*(D23), 8645, doi:10.1029/2002JD003226.

Baltensperger, U., M. Schwikowski, D. T. Jost, S. Nyeki, H. W. Gaggeler, and O. Poulida (1998), Scavenging of atmospheric constituents in mixed phase clouds at the high-alpine Junfraujoch part I: Basic concept and aerosol scavenging by clouds, *Atmos. Environ.*, *32*, 3975–3983.

Bassett, M., and J. H. Seinfeld (1984), Atmospheric equilibrium model of sulfate and nitrate aerosols, II. Particle size analysis, *Atmos. Environ.*, *18*, 1163–1170.

Bates, T. S., et al. (2006), Aerosol direct radiative effects over the northwest Atlantic, northwest Pacific, and North Indian Oceans: Estimates based on in-situ chemical and optical measurements and chemical transport modeling, *Atmos. Chem. Phys. Disc.*, *6*, 175–362.

Baumann, K., F. Ift, J. Z. Zhao, and W. L. Chameides (2003), Discrete measurements of reactive gases and fine particle mass and composition during the 1999 Atlanta Supersite Experiment, *J. Geophys. Res.*, *108*(D7), 8416, doi:10.1029/2001JD001210.

Baynard, T., R. M. Garland, A. R. Ravishankara, M. A. Tolbert, and E. R. Lovejoy (2006), Key factors influencing the relative humidity dependence of aerosol light scattering, *Geophys. Res. Lett.*, *33*, L06813, doi:10.1029/2005GL024898.

Brock, C. A., et al. (2004), Particle characteristics following cloud-modified transport to North America, *J. Geophys. Res.*, *109*, D23S26, doi:10.1029/2003JD004198.

Broekhuizen, K., P. P. Kumar, and J. P. D. Abbatt (2004), Partially soluble organics as cloud condensation nuclei: Role of trace soluble and surface active species, *Geophys. Res. Lett.*, *31*, L01107, doi:10.1029/2003GL018203.

Brown, S. S., et al. (2006), Variability in nocturnal nitrogen oxide processing and its role in regional air quality, *Science*, *311*, 67–70.

Chirico, R. D., W. V. Steele, A. Nguyen, T. D. Klots, and S. E. Knipmeyer (1996), Thermodynamic properties of pyridine. 1. Vapor pressures, high-temperature heat capacities, densities, critical properties, derived thermodynamic functions, vibrational assignment, and derivation of recommended values, *J. Chem. Thermodyn.*, *28*, 797–818.

Clarke, A. D. (1993), Atmospheric nuclei in the Pacific midtroposphere: Their nature, concentration and evolution, *J. Geophys. Res.*, *98*, 20,633–20,647.

Cornell, S. E., T. D. Jickells, J. N. Cape, and R. A. Duce (2003), Organic nitrogen deposition on land and coastal environments: A review of methods and data, *Atmos. Environ.*, *37*, 2173–2191.

Cziczo, D. J., P. J. DeMott, S. D. Brooks, A. J. Prenni, D. S. Thomson, D. Baumgardner, J. C. Wilson, S. M. Kreidenweis, and D. M. Murphy (2004), Observations of organic species and atmospheric ice formation, *Geophys. Res. Lett.*, *31*, L12116, doi:10.1029/2004GL019822.

Dibb, J. E., R. W. Talbot, E. M. Scheuer, G. Seid, M. A. Avery, and H. B. Singh (2003), Aerosol chemical composition in Asian continental outflow during the TRACE-P campaign: Comparison with PEM-West B, *J. Geophys. Res.*, *108*(D21), 8815, doi:10.1029/2002JD003111.

Eisele, F. L. (1988), First tandem mass spectrometric measurement of tropospheric ions, *J. Geophys. Res.*, *93*, 716–724.

Ervens, B., G. Feingold, G. J. Frost, and S. M. Kreidenweis (2004), A modeling study of aqueous production of dicarboxylic acids: 1. Chemical pathways and speciated organic mass production, *J. Geophys. Res.*, *109*, D15205, doi:10.1029/2003JD004387.

Facchini, M. C., et al. (1999), Partitioning of the organic aerosol component between fog droplets and interstitial air, *J. Geophys Res.*, *104*, 26,821–26,832.

Faude, F., and J. Goschnick (1997), XPS, SIMS and SNMS applied to a combined analysis of aerosol particles from a region of considerable air pollution in the upper Rhine valley, *Fresenius J. Anal. Chem.*, *358*, 67–72.

Gard, E. E., et al. (1998), Direct observation of heterogeneous chemistry in the atmosphere, *Science*, *279*, 1184–1188.

Garland, R. M., M. E. Wise, M. R. Beaver, H. L. DeWitt, A. C. Aiken, J. L. Jimenez, and M. A. Tolbert (2005), Impact of palmitic acid coating on the water uptake and loss of ammonium sulfate particles, *Atmos. Chem. Phys.*, *5*, 1951–1961.

Haggerstone, A.-L., L. J. Carpenter, N. Carslaw, and G. McFiggans (2005), Improved model predictions of HO_2 with gas to particle mass transfer rates calculated using aerosol number size distributions, *J. Geophys. Res.*, *110*, D04303, doi:10.1029/2004JD005282.

Heald, C. L., D. J. Jacob, R. J. Park, L. M. Russell, B. J. Huebert, J. H. Seinfeld, H. Liao, and R. J. Weber (2005), A large organic aerosol source in the free troposphere missing from current models, *Geophys. Res. Lett.*, *32*, L18809, doi:10.1029/2005GL023831.

Hegg, D. A., J. Livingston, P. V. Hobbs, T. Novakov, and P. Russell (1997), Chemical apportionment of aerosol column optical depth off the mid-Atlantic coast of the United States, *J. Geophys. Res.*, *102*, 25,293–25,303.

Hudson, P. K., D. M. Murphy, D. J. Cziczo, D. S. Thomson, J. A. deGouw, C. Warneke, J. Holloway, H.-J. Jost, and G. Hübler (2004), Biomass burning particle measurements: Characteristic composition and chemical processing, *J. Geophys. Res.*, *109*, D23S27, doi:10.1029/2003JD004398.

Huebert, B. J., S. G. Howell, L. Zhuang, J. A. Heath, M. R. Litchy, D. J. Wylie, J. L. Kreidler-Moss, S. Coppicus, and J. E. Pfeiffer (1998), Filter and impactor measurements of anions and cations during the First Aerosol Characterization Experiment (ACE 1), *J. Geophys. Res.*, *103*, 16,493–16,509.

Jayne, J. T., D. C. Leard, X. Zhang, P. Davidovits, K. A. Smith, C. E. Kolb, and D. R. Worsnop (2000), Development of an aerosol mass spectrometer for size and composition analysis of submicron particles, *Aerosol Sci. Technol.*, *33*, 49–70.

Jimenez, J. L., et al. (2003), Ambient aerosol sampling using the Aerodyne Aerosol Mass Spectrometer, *J. Geophys. Res.*, *108*(D7), 8425, doi:10.1029/2001JD001213.

Jost, H. J., et al. (2004), Observations of mid-latitude forest fire plumes in the stratosphere, *Geophys. Res. Lett.*, *31*, L11101, doi:10.1029/2003GL019253.

Kelly, J. T., and A. S. Wexler (2005), Thermodynamics of carbonates and hydrates related to heterogeneous reactions involving mineral aerosol, *J. Geophys. Res.*, *110*, D11201, doi:10.1029/2004JD005583.

Kinne, S., et al. (2005), An AeroCom initial assessment—Optical properties in aerosol component modules of global models, *Atmos. Chem. Phys. Disc.*, *5*, 8285–8330.

Kline, J., B. Huebert, S. Howell, B. Blomquist, J. Zhuang, T. Bertram, and J. Carrillo (2004), Aerosol composition and size versus altitude measured from the C-130 during ACE-Asia, *J. Geophys. Res.*, *109*, D19S08, doi:10.1029/2004JD004540.

Krejci, R., J. Ström, M. de Reus, and W. Sahle (2004), Single particle analysis of the accumulation mode aerosol over the northeast Amazonian tropical rain forest, Surinam, South America, *Atmos. Chem. Phys. Disc.*, *4*, 533–568.

Lamarque, J.-F., J. T. Kiehl, P. G. Hess, W. D. Collins, L. K. Emmons, P. Ginoux, C. Luo, and X. X. Tie (2005), Response of a coupled chemistry-climate model to changes in aerosol emissions: Global impact on the hydrological cycle and the tropospheric burdens of OH, ozone, and NO_x, *Geophys. Res. Lett.*, *32*, L16809, doi:10.1029/2005GL023419.

Lazrus, A. L., and B. W. Gandrud (1974), Stratospheric sulfate aerosol, *J. Geophys. Res.*, *79*, 3424–3431.

Lee, S., D. M. Murphy, D. S. Thomson, and A. M. Middlebrook (2002), Chemical components of single particles measured with Particle Analysis by Laser Mass Spectrometry (PALMS) during the Atlanta SuperSite Project: Focus on organic/sulfate, lead, soot, and mineral particles, *J. Geophys. Res.*, *107*(D1), 4003, doi:10.1029/2000JD000011.

Lee, S., D. M. Murphy, D. S. Thomson, and A. M. Middlebrook (2003), Nitrate and oxidized organic ions in single particle mass spectra during the 1999 Atlanta Supersite Project, *J. Geophys. Res.*, *108*(D7), 8417, doi:10.1029/2001JD001455.

Lee, Y. N., et al. (2003), Airborne measurement of inorganic ionic components of fine aerosol particles using the particle-into-liquid sampler coupled to ion chromatography technique during ACE-Asia and TRACE-P, *J. Geophys. Res.*, *108*(D23), 8646, doi:10.1029/2002JD003265.

Li, S. M., and J. W. Winchester (1993), Aerosol silicon and associated elements in the Arctic high and midtroposphere, *Atmos. Environ., Part A*, *27*, 2907–2912.

Liao, J., and J. H. Seinfeld (2005), Global impacts of gas-phase chemistry-aerosol interactions on direct radiative forcing by anthropogenic aerosols and ozone, *J. Geophys. Res.*, *110*, D18208, doi:10.1029/2005JD005907.

Limbeck, A., and H. Puxbaum (2000), Dependence of in-cloud scavenging of polar organic aerosol compounds on the water solubility, *J. Geophys. Res.*, *105*, 19,857–19,867.

Maria, S. F., L. M. Russell, B. J. Turpin, R. J. Porcja, T. L. Campos, R. J. Weber, and B. J. Huebert (2003), Source signatures of carbon monoxide and organic functional groups in Asian Pacific Regional Aerosol Characterization Experiment (ACE-Asia) submicron aerosol types, *J. Geophys. Res.*, *108*(D23), 8637, doi:10.1029/2003JD003703.

Martins, J. V., P. Artaxo, C. Liousse, J. S. Reid, P. V. Hobbs, and Y. J. Kaufman (1998), Effects of black carbon content, particle size, and mixing on light absorption by aerosols from biomass burning in Brazil, *J. Geophys. Res.*, *103*, 32,041–32,050.

McFiggans, G., et al. (2005a), Simplification of the representation of the organic component of atmospheric particulates, *Faraday Disc.*, *130*, 341–362.

McFiggans, G., et al. (2005b), The effect of physical and chemical aerosol properties on warm cloud droplet activation, *Atmos. Chem. Phys. Disc.*, *5*, 8507–8647.

Milne, P. J., and R. G. Zika (1993), Amino acid nitrogen in atmospheric aerosols: Occurrence, sources and photochemical modification, *J. Atmos. Chem.*, *16*, 361–398.

Murphy, D. M., and D. S. Thomson (1997), Chemical composition of single aerosol particles at Idaho Hill: Negative ion measurements, *J. Geophys. Res.*, *102*, 6353–6368.

Murphy, D. M., and D. S. Thomson (2000), Halogen ions and NO+ in the mass spectra of aerosols in the upper troposphere and lower stratosphere, *Geophys. Res. Lett.*, *27*, 3217–3220.

Murphy, D. M., D. S. Thomson, and A. M. Middlebrook (1997), Bromine, iodine, and chlorine in single aerosol particles at Cape Grim, *Geophys. Res. Lett.*, *24*, 3197–3200.

Murphy, D. M., D. S. Thomson, and M. J. Mahoney (1998a), In situ measurements of organics, meteoritic material, mercury, and other elements in aerosols at 5 to 19 kilometers, *Science*, *282*, 1664–1669.

Murphy, D. M., J. R. Anderson, P. K. Quinn, L. M. McInnes, F. J. Brechtel, S. M. Kreidenweis, A. M. Middlebrook, M. Pósfai, D. S. Thomson, and P. R. Buseck (1998b), Influence of sea salt on aerosol radiative properties in the Southern Ocean marine boundary layer, *Nature*, *392*, 62–65.

Murphy, D. M., A. M. Middlebrook, and M. Warshawsky (2003), Cluster analysis of data from the Particle Analysis by Laser Mass Spectrometry (PALMS) instrument, *Aerosol Sci. Technol.*, *37*, 382–391.

Murphy, D. M., D. J. Cziczo, P. K. Hudson, and D. S. Thomson (2006a), Carbonaceous material in aerosol particles in the lower stratosphere and tropopause region, *J. Geophys. Res.*, doi:10.1029/2006JD007297, in press.

Murphy, D. M., P. K. Hudson, D. S. Thomson, P. J. Sheridan, and J. C. Wilson (2006b), Observations of mercury-containing aerosols, *Environ Sci. Technol.*, *40*, 3163–3167.

Neuman, J. A., et al. (2003), Variability in ammonium nitrate formation and nitric acid depletion with altitude and location over California, *J. Geophys. Res.*, *108*(D17), 4557, doi:10.1029/2003JD003616.

Novakov, T., D. A. Hegg, and P. V. Hobbs (1997), Airborne measurements of carbonaceous aerosols on the East Coast of the United States, *J. Geophys. Res.*, *102*, 30,023–30,030.

Okada, K., M. Ikegami, Y. Zaizen, Y. Makino, J. B. Jensen, and J. L. Gras (2001), The mixture state of individual aerosol particles in the 1997 Indonesian haze episode, *J. Aerosol Sci.*, *32*, 1269–1279.

Pastor, S. J., J. O. Allen, L. S. Hughes, P. Bhave, G. R. Cass, and K. A. Prather (2003), Ambient single particle analysis in Riverside, California

by aerosol time-of-flight mass spectrometry during the SCOS97-NARSTO, *Atmos. Environ.*, *37*, suppl. 2, S239–S258.

Popp, P. J., et al. (2004), Nitric acid uptake on subtropical cirrus cloud particles, *J. Geophys. Res.*, *109*, D06302, doi:10.1029/2003JD004255.

Posfai, M., J. R. Anderson, P. R. Buseck, and H. Sievering (1999), Soot and sulfate aerosol particles in the remote marine troposphere, *J. Geophys. Res.*, *104*, 21,685–21,693.

Putaud, J.-P., R. Van Dingenen, A. Dell'Acqua, F. Raes, E. Matta, S. Decesari, M. C. Facchini, and S. Fuzzi (2004), Size-segregated aerosol mass closure and chemical composition in Monte Cimone (I) during MINATROC, *Atmos. Chem. Phys.*, *4*, 889–902.

Quinn, P. K., et al. (2005), Impact of particulate organic matter on the relative humidity dependence of light scattering: A simplified parameterization, *Geophys. Res. Lett.*, *32*, L22809, doi:10.1029/2005GL024322.

Ravishankara, A. R. (2005), Chemistry-climate coupling: The importance of chemistry in climate issues, *Faraday Disc.*, *130*, 9–26.

Schreiner, J., U. Schmid, C. Voigt, and K. Mauersberger (1999), Focusing of aerosols into a particle beam at pressures from 10 to 150 torr, *Aerosol Sci. Technol.*, *31*, 373–382.

Schulte, P., and F. Arnold (1990), Pyridinium ions and pyridine in the free troposphere, *Geophys. Res. Lett.*, *17*, 1077–1080.

Sellegri, K., P. Laj, R. Dupuy, M. Legrand, S. Preunkert, and J.-P. Putaud (2003), Size-dependent scavenging efficiencies of multicomponent atmospheric aerosols in clouds, *J. Geophys. Res.*, *108*(D11), 4334, doi:10.1029/2002JD002749.

Sheridan, P. J., C. A. Brock, and J. C. Wilson (1994), Aerosol particles in the upper troposphere and lower stratosphere: Elemental composition and morphology of individual particles in northern midlatitudes, *Geophys. Res. Lett.*, *21*, 2587–2590.

Sommariva, R., A.-L. Haggerstone, L. J. Carpenter, N. Carslaw, D. J. Creasey, D. E. Heard, J. D. Lee, A. C. Lewis, M. J. Pilling, and J. Zádor (2004), OH and HO_2 chemistry in clean marine air during SOAPEX-2, *Atmos. Chem. Phys.*, *4*, 839–856.

Sullivan, R. C., and K. A. Prather (2005), Recent advances in our understanding of atmospheric chemistry and climate made possible by on-line aerosol analysis instrumentation, *Anal. Chem.*, *77*, 3861–3885.

Tanner, D. J., and F. L. Eisele (1991), Ions in oceanic and continental air masses, *J. Geophys. Res.*, *96*, 1023–1031.

Thomson, D. S., M. E. Schein, and D. M. Murphy (2000), Particle analysis by laser mass spectrometry WB-57F instrument overview, *Aerosol Sci. Technol.*, *33*, 153–169.

Trochkine, D., Y. Iwasaka, A. Matsuki, M. Yamada, Y.-S. Kim, T. Nagatani, D. Zhang, G.-Y. Shi, and Z. Shen (2003), Mineral aerosol particles collected in Dunhuang, China, and their comparison with chemically modified particles collected over Japan, *J. Geophys. Res.*, *108*(23), 8642, doi:10.1029/2002JD003268.

Weber, R. J., D. Orsini, Y. Daun, Y. N. Lee, P. J. Klotz, and F. Brechtel (2001), A particle-into-liquid collector for rapid measurement of aerosol bulk chemical composition, *Aerosol Sci. Technol.*, *35*, 718–727.

Zhang, D., and Y. Iwasaka (2001), Chlorine deposition on dust particles in marine atmosphere, *Geophys. Res. Lett.*, *28*, 3613–3616.

Ziereis, H., et al. (2004), Uptake of reactive nitrogen on cirrus cloud particles during INCA, *Geophys. Res. Lett.*, *31*, L05115, doi:10.1029/2003GL018794.

Zobrist, B., et al. (2006), Oxalic acid as a heterogeneous ice nucleus in the upper troposphere and its indirect aerosol effect, *Atmos. Chem. Phys.*, *6*, 3115–3129.

D. J. Cziczo, Eidgenössische Technische Hochschule, CH-8092 Zurich, Switzerland.

K. D. Froyd, A. M. Middlebrook, D. M. Murphy, and D. S. Thomson, Earth System Research Laboratory, NOAA, Boulder, CO 80305, USA. (daniel.m.murphy@noaa.gov)

P. K. Hudson, Department of Chemistry, University of Iowa, Iowa City, IA 52242, USA.

B. M. Matthew, Hach Company, Loveland, CO 80539, USA.

R. E. Peltier, A. Sullivan, and R. J. Weber, School of Earth and Atmospheric Sciences, Georgia Institute of Technology, Atlanta, GA 30332, USA.